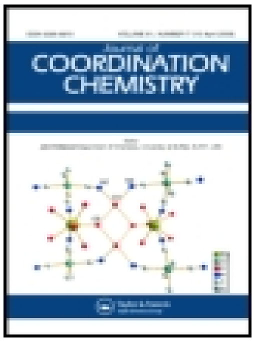

Journal of Coordination Chemistry

ISSN: 0095-8972 (Print) 1029-0389 (Online) Journal homepage: http://www.tandfonline.com/loi/gcoo20

Theoretical investigation on molecular structure of a new mononuclear copper(II) thiocyanato complex with tridentate Schiff base ligand

Santarupa Thakurta, Ray. J. Butcher, Antonio Frontera & Samiran Mitra

To cite this article: Santarupa Thakurta, Ray. J. Butcher, Antonio Frontera & Samiran Mitra (2017): Theoretical investigation on molecular structure of a new mononuclear copper(II) thiocyanato complex with tridentate Schiff base ligand, Journal of Coordination Chemistry, DOI: 10.1080/00958972.2017.1394460

To link to this article: http://dx.doi.org/10.1080/00958972.2017.1394460

Publisher: Taylor & Francis
Journal: *Journal of Coordination Chemistry*
DOI: http://doi.org/10.1080/00958972.2017.1394460

Theoretical investigation on molecular structure of a new mononuclear copper(II) thiocyanato complex with tridentate Schiff base ligand

SANTARUPA THAKURTA*[a], RAY. J. BUTCHER[b], ANTONIO FRONTERA[c] and SAMIRAN MITRA*[d,e]

[a]Department of Chemistry, Prabhu Jagatbandhu College, Howrah - 711302, India
[b]Department of Chemistry, Howard University, 2400 Sixth Street NW, Washington, DC 20059, USA
[c]Departament de Química, Universitat de les Illes Balears, Crta de Valldemossa km 7.5, 07122 Palma de Mallorca (Baleares), Spain
[d]Department of Chemistry, Jadavpur University, Kolkata - 700032, India
[e]Department of Chemistry, Heritage Institute of Technology, Kolkata - 700107, India

An asymmetrical Schiff base ligand, 4-bromo-2-(2-pyridylmethyliminomethyl)phenol (HL), and its copper(II) complex, [Cu(L)(SCN)] (**1**), have been synthesized. Complex **1** is experimentally characterized by elemental analysis, FT-IR and UV-vis spectroscopic techniques, and cyclic voltammetry. The structure of the complex has been established by single-crystal X-ray diffraction studies, which reveal a square planar geometry of the central copper(II) ion in **1**. The neighboring molecules of the complex connect each other by π-π stacking interactions with centroid-to-centroid ring distance 3.653 Å. The ligand can display two possible tautomeric forms; therefore **1** can have an alternate molecular structure. DFT calculations have been employed to investigate the structure and relative stabilities of the suggested tautomeric forms of the ligand and its corresponding copper(II) complex.

Keywords: Schiff base; Copper(II) complex; Crystal structure; Tautomer stability; DFT Calculations

1. Introduction

Transition metal complexes with oxygen and nitrogen donor Schiff bases have been extensively studied because they play an important role in the coordination chemistry related to catalysis and

---

*Corresponding authors. Email: sthakurtaju@yahoo.co.in (S. Thakurta); samiranju92@gmail.com (S. Mitra) enzymatic reactions [1-4], magnetism [5, 6] and supramolecular architectures [7-9]. The azomethine linkage in Schiff bases is responsible for their antibacterial, antiviral, and antifungal activities [10]. Tridentate Schiff bases with NNO-donor sets have been preferred by inorganic chemists because such ligands can effectively act as chelate leaving the metal ion coordinatively unsaturated. In order to satisfy the coordination number of metal ions preferring square planar, square pyramidal and octahedral geometry, different auxiliary ligands (N_3^-, NCO^-, NCS^-, CN^-, acetate, carboxylate, oxalate, halogen) have been employed. Among them, pseudohalide ligands can coordinate to transition metal atoms in different ways, for example as a terminal ligand or as a bridge (end-to-end/end-on fashion) giving rise to interesting molecular topologies and crystal packing motifs. Our research group previously reported several mono- and multinuclear transition metal complexes with tridentate Schiff base ligands in the presence of coordinating N_3^-, NCO^-, NCS^- anions [11-14] and their possible magnetic, catalytic or biological applications. In continuation to our earlier studies, we have synthesized an unsymmetrical NNO-donor Schiff base ligand (HL) from the condensation of 5-bromosalicylaldehyde and 2-picolylamine and monitored its coordination behavior towards copper(II) ion in combination with thiocyanate anion as a coligand (scheme 1). This paper describes the synthesis, elemental analyses, spectroscopic studies and electrochemical properties of a new mononuclear complex, [Cu(L)SCN] (**1**).

Interestingly, HL can present an additional tautomeric form denoted as HL' (scheme 2), which can provide an alternative molecular structure for the copper(II) complex. Identification of the influence of tautomerism on chemical and biological properties of molecules is a significant task in pharmacophore-based virtual screening and drug discovery program [15, 16]. Recently, DFT methods are found to be effective to study the tautomeric forms of heterocyclic compounds [17-19]. There are few reports on combined theoretical and experimental analysis of Schiff bases displaying two possible tautomeric forms, the enol-imine (OH) and the keto-amine (NH) [20, 21]. But theoretical studies on tautomeric forms of metal complexes of Schiff base ligands are still very rare [22]. The aim of the present work is to predict the relative tautomer stabilities of the ligand and the complex using the total energies and thermodynamic parameters obtained from the DFT/B3LYP calculations. Herein, the theoretical results obtained have been nicely correlated with the structural features of the complex.

2. Experimental

2.1. *Materials and physical measurements*

All the chemicals and solvents employed for the syntheses were of analytical grade. 5-Bromosalicylaldehyde and 2-picolylamine (or 2-aminomethylpyridine) were purchased from Aldrich Co., USA and $Cu(NO_3)_2{\cdot}3H_2O$ was from Merck India Ltd. Sodium thiocyanate (Aldrich, USA) was used as received.

The Fourier transform infrared spectra (4000-200 cm^{-1}) of the ligand and the complex were recorded on a Perkin Elmer Spectrum RX I FT-IR system with solid KBr disc. The electronic spectra were recorded on a Perkin Elmer Lambda-40 UV/Vis spectrophotometer using HPLC grade acetonitrile as solvent. C, H and N microanalyses were carried out with a Perkin Elmer 2400 II elemental analyser. Electrochemical measurements of the complex were performed on a VersaStat-PotentioStat II cyclic voltammeter, using HPLC grade acetonitrile as solvent with 0.1(M) tetrabutylammonium perchlorate as supporting electrolyte, at a scan rate of 0.1 V/s. Platinum and saturated calomel electrode (SCE) were the working and the reference electrodes in the process, respectively.

2.2. *Synthesis*

2.2.1. Synthesis of the Schiff base ligand. HL was prepared following a method reported [23]. 25 mL methanolic solution of 2-picolylamine (5 mmol, 0.54 g) was added to an equivolume methanolic solution of 5-bromosalicylaldehyde (5 mmol, 1.00 g). The mixture was refluxed for 2 h after which a yellow solution resulted, indicating formation of the Schiff base. The reaction mixture was then allowed to stand at room temperature for two days to yield yellow crystals. Anal. Calc. (%) for $C_{13}H_{11}BrN_2O$: C, 53.63; H, 3.81; N, 9.62. Found (%): C, 53.59; H, 3.77; N, 9.58.

2.2.2. Synthesis of the complex. A methanolic solution of HL (0.291 g, 1 mmol) was added dropwise to a clear solution of $Cu(NO_3)_2{\cdot}3H_2O$ (0.930 g, 1 mmol) in 25 mL methanol and immediately an intense blue color developed. The solution was heated to boiling followed by the addition of sodium thiocyanate (0.81 g, 1 mmol) in a minimum volume of methanol. The solution, on being concentrated in the open atmosphere, yielded olive-green rectangular plate shaped single-crystals after five days. Anal. Calc. (%) for $C_{14}H_{10}BrCuN_3OS$ (FW: 411.76): C, 40.85; H, 2.45; N, 10.20. Found (%): C, 40.83; H, 2.41; N, 10.18%.

2.3. *Crystal structure determination*

A diffraction-quality single-crystal of **1** was mounted on an Oxford Diffraction Gemini diffractometer equipped with a graphite monochromator and Cu-$K\alpha$ radiation (λ = 1.5418 Å). Intensity data were collected at 200(2) K using the ω scan technique and multi-scan absorption correction was applied to the intensity values empirically. Data collection, unit cell refinement and data reduction were performed using CrysAlisRED software [24]. The structure of the complex was solved by direct-method procedures with SHELXS-97 [25] and refined by full-matrix least-squares based on F^2 with SHELXL-97 [26]. The non-hydrogen atoms were refined with anisotropic factors. All hydrogens were positioned geometrically treated as riding on the bound atom. All crystallographic computations and graphical works were carried out using PLATON99 [27] and ORTEP [28]. A summary of the crystallographic data and details of the structure refinements are listed in table 1.

2.4. *Theoretical methods*

The geometries of ligands and complexes studied herein have been fully optimized by Gaussian09 software package [29] which was used for calculations and modeling the considered molecules. Molecular structures of both the ligand and the complex along with their tautomeric forms were optimized at the B3LYP/6-311+G* [30] level of theory. Vibrational frequency calculations have been performed after optimization and no imaginary frequencies were identified. At first, all calculations are performed in gas phase and then in solution (MeOH) by means of the Polarizable Continuum Model (PCM), which uses the integral equation formalism variant (IEFPCM) [31]. The HOMO-LUMO plots have been generated using Gaussview.

3. Results and discussion

The Schiff base ligand, 4-bromo-2-(2-pyridylmethyliminomethyl)phenol (HL), which is used to synthesize **1**, has been structurally characterized by Zhang *et al.* [23] and the crystal structure is shown in figure S1. The ligand crystallizes in the triclinic space group, *P*1, with cell dimensions a = 4.4740(10) Å, b = 9.529(2) Å, c = 14.271(2) Å, α = 92.650(10)°, β = 93.720(10)° and γ =

95.16(2)°. The imine nitrogen atom is found to be engaged in intramolecular hydrogen-bonding with the phenol group (N...H = 1.87 Å). Two molecules are linked by an intermolecular Br…N(py) interaction of 3.263(4) Å across an inversion center, forming a dimeric entity.

The air-stable single crystals of **1** are synthesized according to the procedure described in scheme 1. The comparison of the solid state infrared spectra of the ligand and the complex clearly indicates the coordination of the deprotonated tridentate ligand to the copper(II) center. The complex is soluble in common organic solvents like CH_3CN, MeOH and DMF. In order to understand the behavior and stability of the complex in solution, the electronic spectrum was recorded and the electrochemical measurements were performed using acetonitrile as solvent. With the help of these studies we can establish that the complex is stable enough to retain its solid state structure, as confirmed by single-crystal X-ray diffraction, in solution phase also.

3.1. *Fourier Transform Infrared spectra*

The formation of the Schiff base ligand has been supported by infrared spectroscopy (figure S2). The absence of characteristic sharp bands at 3340 and 3205 cm^{-1} for the asymmetric and symmetric N–H stretching vibrations confirms the successful condensation of $-NH_2$ functionality of 2-picolylamine. A strong sharp absorption band around 1635 cm^{-1} may be assigned for the azomethine (C=N) stretching frequency. The C-O stretching mode of vibration of phenol group is observed at 1252 cm^{-1}. The peak at 1490 cm^{-1} can be attributed to C=N stretching vibration of pyridine ring. The infrared spectrum of **1** is fully consistent with its single-crystal structure (figure S3). The characteristic azomethine absorption band of the free Schiff base ligand is shifted to 1605 cm^{-1} in the complex. The shifting of this band to lower frequency clearly indicates the coordination of the nitrogen atom of the imine group to the metal ion [32]. The lowering of phenolic C-O stretching frequency to 1220 cm^{-1} in the spectrum of the complex provides evidence for coordination to the metal ion through the deprotonated phenolic oxygen atom. Ligand coordination to metal center is substantiated by prominent bands at 455 and 375 cm^{-1} which can be attributed to ν(M-N) and ν(M-O), respectively. The spectrum of free Schiff base shows a weak, broad band at 3000-3400 cm^{-1} due to hydrogen-bonded enolic O-H group which disappears in the IR spectrum of the complex, indicating deprotonation of the Schiff base ligand upon complexation. The sharp single peak at 2084 cm^{-1} corresponds to the N-bonded thiocyanate group [33].

3.2. *Electronic spectra*

The electronic spectral data for **1** in HPLC grade acetonitrile solvent are in good agreement with its geometry. Complex **1** shows a broad band centered at 615 nm which is a typical *d-d* band for Cu^{II} in square-planar environment [34]. The strong absorption band at 385-395 nm can be attributed to the charge-transfer transition from the coordinated unsaturated ligand to the metal ion (LMCT) [35]. The intense high-energy bands at about 262 and 288 nm may be assigned to the intraligand $\pi\rightarrow\pi^*$ and $n\rightarrow\pi^*$ transitions, respectively. The electronic spectrum is shown in figure S4.

3.3. *Electrochemical study*

The electrochemical behavior of **1** was studied using acetonitrile as solvent at a scan rate of 100 mVs^{-1} with tetrabutylammonium perchlorate as supporting electrolyte. Complex **1** (figure 1) shows one reductive response on the negative side of SCE at -0.85 V. This is assigned to the reduction of Cu(II) to Cu(I). During the anodic scan, it shows a reversible oxidative response at -0.78 V, assigned to the Cu(I)→Cu(II) oxidation. The peak-to-peak separation of 70 mV suggests the reversible nature of the redox reaction for Cu(II)/Cu(I). The reversible nature of the redox process is also evident from the almost unit value of the ratio of cathodic peak and anodic peak current (i_{pc}/i_{pa}) [36]. The features of the cyclic voltammogram of **1** corroborate with the square planar geometry of the copper(II) atom as observed in the X-ray structural analysis [37].

3.4. *Crystal structure of [Cu(L)SCN] (1)*

The perspective view of **1** with the atom labeling scheme is shown in figure 2. The crystal structure features a four-coordinate copper center surrounded by two nitrogen atoms and one deprotonated oxgyen atom of the tridentate NNO donor Schiff base ligand. The N-coordinated thiocyanato ligand completes the coordination of the Cu(II) center to a square planar geometry. In **1**, the pyridine nitrogen atom (N2) is located *trans* to the deprotonated enolato oxygen (O) of the Schiff base ligand whereas the imine nitrogen atom (N1) of $[L]^-$ and the thiocyanate nitrogen atom (N) occupy the other *trans* positions. However, the square plane is slightly distorted, which is manifested in the deviations of *trans* angles from 180° and *cis* angles from 90° (table 2). A certain 'twisting' of the square can be interpreted as a minor distortion towards tetrahedral geometry. Thus, the dihedral angle between the two planes N1/Cu/N2 and O/Cu/N is 3.34°, as compared with 0° for a perfectly square-planar arrangement and 90° for a perfect tetrahedral arrangement. The central copper atom is deviated from the mean plane defined by N1, N2, O and N atoms by 0.036 Å only. The terminal thiocyanate ligand which is bound through its nitrogen atom is almost linear and shows a bent coordination mode with the metal [N–C–S/Cu–N–C = 179.65/165.09)°]. The chelate bite angles in the five-membered and six-membered rings formed by the coordination of pyridine-N and the imine-N, and enolato-O and imine-N of the tridentate Schiff base $[L]^-$ to the copper(II) center are 82.83(8)° and 93.17(7)°, respectively. Both of these five- and the six-membered chelate rings lie almost in the same plane with an angle of 2.94° between them. The fact that Cu–N(pyridine) bond is longer than Cu–N(imine) bond despite the presence of same sp^2 hybridized nitrogen can be attributed to the delocalization of electrons in the six-membered chelate ring. The Cu-N(thiocyanato) bond length is in agreement with the reported literature values for similar complexes [38]. In the solid state, π-π stacking interactions are present involving the pyridine and phenolic rings of the neighboring molecules as depicted in the packing diagram of the complex (figure 3). The inter-unit Cu…Cu distance is 3.772 Å and the corresponding centroid-to-centroid ring distance (3.653 Å) is as expected for stacks [39]. The packing diagram also reveals the presence of intermolecular Br…S halogen bond (3.48 Å) [40, 41]. Selected bond lengths and angles of **1** are summarized in table 2.

3.5. *Theoretical study*

According to the calculated relative energies, the HL ligand is by 2.7 kcal/mol and 2.3 kcal/mol more stable than its tautomeric form denoted as HL’ in gas phase and in MeOH solution, respectively (figure 4a,b). Since the hydrogen atom involved in the tautomeric equilibrium (scheme 2) is not acidic, the kinetic barrier for HL–HL’ transformation should be very high. The higher stability of HL can be rationalized by taking into consideration the intramolecular hydrogen bonding interactions. In the case of HL, in addition to the strong O–H…N hydrogen bond (1.76 Å), a weaker C–H…N(py) hydrogen bond is also established (2.75 Å). This ancillary H-bond is not formed in the tautomeric form HL’ because the rigid C=N bond cannot rotate and, consequently, the approximation of the H-bond acceptor group (N atom of pyridine) is not possible. In addition, the X-ray structure of the ligand which is available from the literature [23] corresponds to the HL tautomeric form (figure S1). The similarity between the experimental and theoretical geometries of HL is exemplified by the identical C=N$_{\mathrm{imine}}$ distance (1.27 Å) and also by the similar N…O distance of the intramolecular O–H…N hydrogen bond (experimental: 2.595 Å, theoretical: 2.62 Å). However, in the solid state the molecule establishes contacts with neighboring molecules. So, the intramolecular C–H…N(py) hydrogen bond is replaced by intermolecular N(py)…Br# halogen bond (# = 1-x, 1-y, 1-z).

In the case of the copper(II) complexes, the energy difference increases to 14.0 kcal/mol in gas phase and 10.9 kcal/mol in solution (figure 4c,d), indicating [Cu(L)SCN] to be more stable than [Cu(L')SCN]. These results are in agreement with the crystallographic data of the complex. The main difference is that the planarity of the [Cu(L)SCN] complex is completely lost in its tautomeric form [Cu(L')SCN], which explains the large energetic difference between the two isomers. The loss of planarity in [Cu(L')SCN] is caused by the presence of the *sp*^{3}-hybridized C atom in the six-membered chelate ring (figure 4d). On the contrary, if the *sp*^{3}-hybridized C atom (C8) is located in the five-membered chelate ring, the system is planar as observed experimentally in **1**. The planarity of the system is convenient in terms of the ability of the ligand to coordinate to the square planar copper(II) center.

In addition, the HOMO-LUMO plots of the tautomeric forms of the ligand have been computed. In the case of HL (figure 5a), both molecular orbitals are mainly located at the bromo-salicylaldimine part of the ligand and the HOMO-LUMO gap is 4.409 eV. In the case of the tautomeric form HL' (figure 5b), the HOMO (-6.132 eV) is also located at the bromo-salicyl moiety and is higher in energy than the HOMO of HL (-6.206 eV), indicating that the latter is more stable, which is in agreement with the energetic results commented above. Finally, the HOMO-LUMO gap is smaller in HL' (3.805 eV) compared to HL, which is also an indication that HL is kinetically more stable than HL'. Similarly, we have also computed the HOMO-LUMO plots for the copper(II) complex using both possible tautomeric forms for the ligand (figure 6) and the behavior is similar to that found for the ligand. In the case of [Cu(L)SCN], both molecular orbitals are mainly located at the bromo-salicylaldimine part of the ligand and the HOMO-LUMO gap is 3.824 eV (figure 6a). In the case of the tautomeric form [Cu(L')SCN] (figure 6b), the HOMO (-5.603 eV) is also located at the bromo-salicyl moiety and is higher in energy than the HOMO of HL (-6.100 eV), indicating that the latter is more stable, which is in agreement with the energetic results commented above. The HOMO-LUMO gap is lower in

[Cu(L')SCN] (1.989 eV) compared to [Cu(L)SCN], which is also an indication that the latter is kinetically more stable than the former.

4. Conclusion

This paper presents a combined theoretical and experimental study of a new mononuclear square planar copper(II)-Schiff base complex. The tautomer stabilities of the free ligand as well as the corresponding copper(II) complex have been calculated using DFT/B3LYP method in gas phase and in solution (MeOH). Between the two suggested tautomeric forms of the complex, the one which is experimentally observed in the X-ray crystallographic structure is found to be more favorable thermodynamically. The predominance of one tautomer over the other can be explained by considering the structural features. Thus, it can be concluded that intramolecular hydrogen-bonding interaction favors the HL structure for free ligand and the planarity factor plays a crucial role in the case of the copper(II) complex [Cu(L)SCN]. Further research can explore the effect of tautomer identity on the pharmacokinetic and pharmacodynamic behaviors of such complexes. Moreover, square planar copper(II) complexes derived from NNO-Schiff bases have recognized cytotoxic activities against selective human cancer cell lines that are both cisplatin sensitive and resistant [42, 43]. So [Cu(L)SCN], chelated by a tridentate Schiff base containing phenolic and pyridine rings as coordinating groups, is expected to show cytotoxicity and DNA cleaving properties [44].

Supplementary material

CCDC 1514288 contains the supplementary crystallographic data for **1**. These data can be obtained free of charge via http://www.ccdc.cam.ac.uk/conts/retrieving.html, or from the Cambridge Crystallographic Data Center, 12 Union Road, Cambridge CB2 1EZ, UK; Fax: (+44) 1223 336 033; or E-mail: deposit@ccdc.cam.ac.uk.

Acknowledgement

S. Thakurta gratefully acknowledges Jadavpur University, Kolkata, India for supporting this study. A. Frontera thanks the MINECO of SPAIN (project CTQ2014-57393-C2-1-P, FEDER funds) for funding and the CTI (UIB) for free allocation of computer time.

Disclosure statement

No potential conflict of interest was reported by the authors.

References

[1] G.A. Morris, H. Zhou, C.L. Stern, S.T. Nguyen. *Inorg. Chem.*, **40**, 3222 (2001).

[2] T. Katsuki. *Coord. Chem. Rev.*, **140**, 189 (1995).

[3] R.L. Lieberman, A.C. Rosenzweig. *Nature*, **434**, 177 (2005).

[4] E.I. Solomon, U.M. Sundaram, T.E. Machonkin. *Chem. Rev.*, **96**, 2563 (1996).

[5] J.R. Friedman, M.P. Sarachik, J. Tejada, R. Ziolo. *Phys. Rev. Lett.*, **76**, 3830 (1996).

[6] L. Thomas, L. Lionti, R. Ballou, D. Gatteschi, R. Sessoli, B. Barbara. *Nature*, **383**, 145 (1996).

[7] P. Day. *J. Chem. Soc., Dalton Trans.*, 701 (1997).

[8] S.L. Castro, Z.M. Sun, C.M. Grant, J.C. Bollinger, D.N. Hendrickson, G. Christou. *J. Am. Chem. Soc.*, **120**, 2365 (1998).

[9] J.-P. Costes, R. Gheorghe, M. Andruh, S. Shova, J.-M.C. Juand. *New J. Chem.*, **30**, 572 (2006).

[10] S. Chandra, X. Sangeetika. *Spectrochim. Acta, Part A*, **60**, 147 (2004).

[11] P. Talukder, A. Datta, S. Mitra, G. Rosair, M.S. El Fallah, J. Ribas. *Dalton Trans.*, 4161 (2004).

[12] S. Banerjee, S. Mondal, W. Chakraborty, S. Sen, R. Gachhui, R.J. Butcher, A.M.Z. Slawin, C. Mandal, S. Mitra. *Polyhedron*, **28**, 2785 (2009).

[13] A. Ray, G.M. Rosair, G. Pilet, B. Dede, C.J. Gomez-Garcia, S. Signorella, S. Bellu, S. Mitra. *Inorg. Chim. Acta*, **375**, 20 (2011).

[14] D. Sadhukhan, C. Rizzoli, E. Garribba, C.J. Gómez-García, A. Yahia-Ammar, L.J. Charbonniere, S. Mitra. *Dalton Trans.*, **41**, 11565 (2012).

[15] J.B. Nanubolu, B. Sridhar, K. Ravikumar. *Cryst. Eng. Comm.*, **16**, 10602 (2014).

[16] S. Ghosh, P.P. Bag, C.M. Reddy. *Cryst. Growth Des.*, **11**, 3489 (2011).

[17] H. Zheng, D. Zhao, Z. Yang. *Chin. J. Chem.*, **29**, 2243 (2011).

[18] S.I. Okovytyy, L.K. Sviatenko, A.A. Gaponov, L.I. Kasyan, I.N. Tarabara, J. Leszczynski. *Eur. J. Org. Chem.*, 280 (2010).

[19] M.V. Sigalov. *J. Phys. Chem. A*, **119**, 1404 (2015).

[20] T. Dziembowska, M. Szafran, A. Katrusiak, Z. Rozwadowski. *J. Mol. Struct.*, **929**, 32 (2009).

[21] E. Temel, C. Alaşalvar, H. Eserci, E. Agar. *J. Mol. Struct.*, **1128**, 5 (2017).

[22] A. Karahan, S. Karabulut, H. Dal, R. Kurtaran, J. Leszczynski. *J. Mol. Struct.*, **1093**, 1 (2015).

[23] Y. Zhang, L.E. Khoo, S.W. Ng. *Acta Cryst.*, **E59**, o1496 (2003).

[24] Oxford Diffraction. *CrysAlis PRO and CrysAlis RED Oxford Diffraction Ltd*., Oxfordshire, England (2007).

[25] G.M. Sheldrick, *SHELXS-97, Program for crystal structure determination*, University of Göttingen, Germany (1997).

[26] G.M. Sheldrick, *SHELXL-97*, *Program for crystal structure refinement*, University of Göttingen, Germany (1997).

[27] A.L. Spek, *PLATON, Molecular Geometry Program*, University of Utrecht, The Netherlands (1999).

[28] L.J. Farrugia, *ORTEP3 for Windows*. *J. Appl. Crystallogr.*, **30**, 565 (1997).

[29] M.J. Frisch, *Gaussian 09*, Revision C.01 (2010).

[30] C. Lee, W. Yang, R.G. Parr. *Phys. Rev.*, **37**, 785 (1988).

[31] J. Tomasi, B. Mennucci, R. Cammi. *Chem. Rev.*, **105**, 2999 (2005).

[32] S.H. Rahaman, R. Ghosh, T.-H. Lu, B.K. Ghosh. *Polyhedron*, **24**, 1525 (2005).

[33] M. Maiti, D. Sadhukhan, S. Thakurta, E. Zangrando, G. Pilet, A. Bauza, A. Frontera, B. Dede, S. Mitra. *Polyhedron*, **75**, 40 (2014).

[34] A.B.P. Lever, *Inorganic electronic spectroscopy, 2nd Edn*., Elsevier, Amsterdam (1984).

[35] P. Dapporto, M. Formica, V. Fusi, L. Giothi, M. Micheloni, P. Paoli, R. Pontellini, P. Rossi. *Inorg. Chem.*, **40**, 6186 (2001).

[36] D.X. West, E. Liberta, S.B. Padhye, R.C. Chikate, P.B. Sonawave, A.S. Kumbrar, R.S. Yerravda. *Coord. Chem. Rev.*, **123**, 49 (1993).

[37] S. Itoh, N. Kishikawa, T. Suzuki, H.D. Takagi. *Dalton Trans.*, 1066 (2005).

[38] S. Chattopadhyay, M.G.B. Drew, A. Ghosh. *Inorg. Chim. Acta*, **359**, 4519 (2006).

[39] C. Janiak. *J. Chem. Soc*., *Dalton Trans.*, 3885 (2000).

[40] G. Cavallo, P. Metrangolo, R. Milani, T. Pilati, A. Priimagi, G. Resnati, G. Terraneo. *Chem. Rev.*, **116**, 2478 (2016).

[41] M.C. Ford, M. Saxton, P.S. Ho. *J. Phys. Chem. Lett.*, **8**, 4246 (2017).

[42] S. Roy, P.U. Maheswari, M. Lutz, A.L. Spek, H. den Dulk, S. Barends, G.P. van Wezel, F. Hartl, J. Reedijk. *Dalton Trans.*, 10846 (2009).

[43] S. Gama, F. Mendes, F. Marques, I.C. Santos, M.F. Carvalho, I. Correia, J.C. Pessoa, I. Santos, A.J. Paulo. *Inorg. Biochem.*, **105**, 637 (2011).

[44] P.U. Maheswari, S. Roy, H. Den Dulk, S. Barends, G. Van Wezel, B. Kozlevcar, P. Gamez, J. Reedijk. *J. Am. Chem. Soc.*, **128**, 710 (2006).

Table 1. Crystallographic data and refinement details for **1**.

Empirical formula	$C_{14}H_{10}BrCuN_3OS$
Formula weight	411.76
Crystal system	Monoclinic
Space group	*P* 21/n
Crystal dimension [mm]	0.41 × 0.34 × 0.12
a (Å)	7.29240(10)
b (Å)	12.30210(10)
c (Å)	16.2658(2)
α (°)	90
β (°)	93.7842(9)
γ (°)	90
V (Å^3)	1456.05(3)
Z	4
T (K)	200(2)
$\lambda_{\text{Cu-K}\alpha}$ (Å)	1.54184
D_c [g cm^{-3}]	1.878
μ (mm^{-1})	6.683
F(000)	812
θ (°)	5.45 to 74.10
Total, Unique data, R_{int}	9571, 2886, 0.0229
Observed data $[I > 2\sigma(I)]$	2561
R, R_w	0.0327, 0.0883
Goodness-of-fit	1.020
$\Delta\rho_{\text{min, max}}$ (e.Å^{-3})	-0.61, 0.63

Table 2. Selected bond distances (Å) and angles (°) for **1**.

Bond lengths		Bond angles	
Cu–O	1.9048(16)	O–Cu–N	89.52(8)
Cu–N1	1.9343(18)	O–Cu–N1	93.17(7)
Cu–N2	2.0062(18)	N–Cu–N2	94.42(8)
Cu–N	1.930(2)	N1–Cu–N2	82.83(8)
N–C	1.156(3)	O–Cu–N2	175.89(8)
S–C	1.620(2)	N–Cu–N1	175.77(8)
C8–N1	1.470(3)	C–N–Cu	165.1(2)
C7–N1	1.282(3)	N–C–S	179.6(2)

Figure captions

Figure 1. Cyclic voltammogram of **1** in acetonitrile solution at a scan rate of 100 mVs^{-1}.

Figure 2. ORTEP view of **1** with atom labeling scheme. Thermal ellipsoids are drawn at the 40% probability level.

Figure 3. Unit cell packing diagram of **1**. Weak interactions are shown as dashed lines.

Figure 4. (a,b): B3LYP/6-311+G* optimized geometries of HL and its tautomeric form HL' and their relative energies both in gas phase and in solution (distances in Å). (c,d): B3LYP/6-311+G* optimized geometries of copper(II) complexes with L^- and its tautomeric form $(L')^-$ and their relative energies both in gas phase and in solution.

Figure 5. (a,b): B3LYP/6-311+G* HOMO-LUMO plots of HL and its tautomeric form HL' and their orbital energies.

Figure 6. (a,b): B3LYP/6-311+G* HOMO-LUMO plots of [Cu(L)SCN] and its tautomeric form [Cu(L')SCN] and their orbital energies.

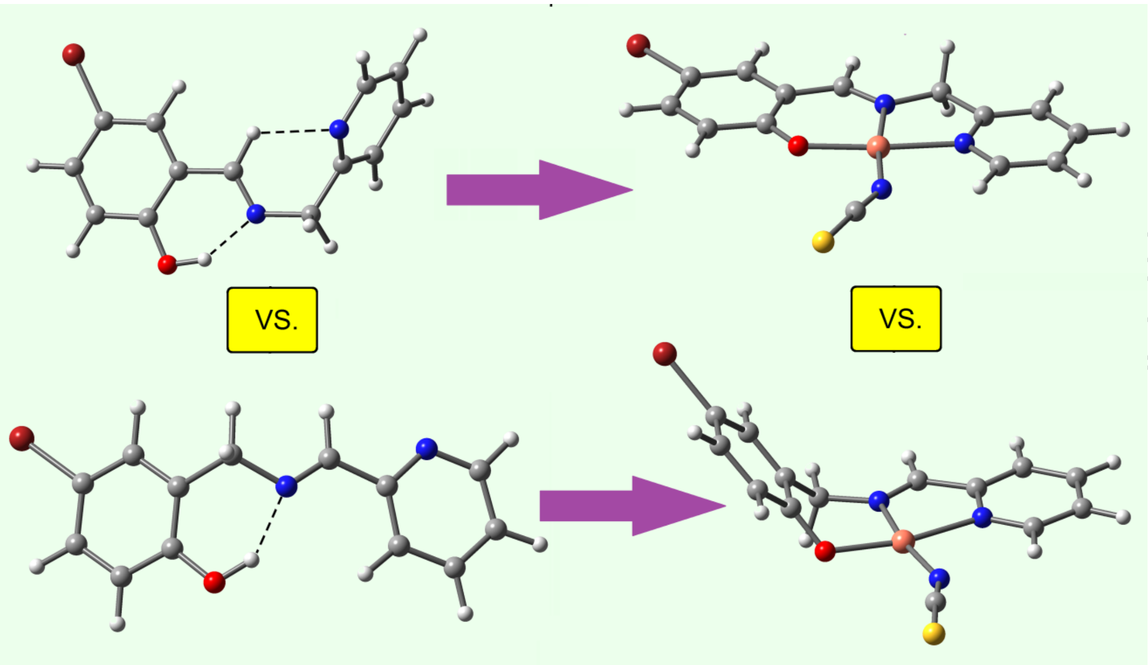
vs.
vs.

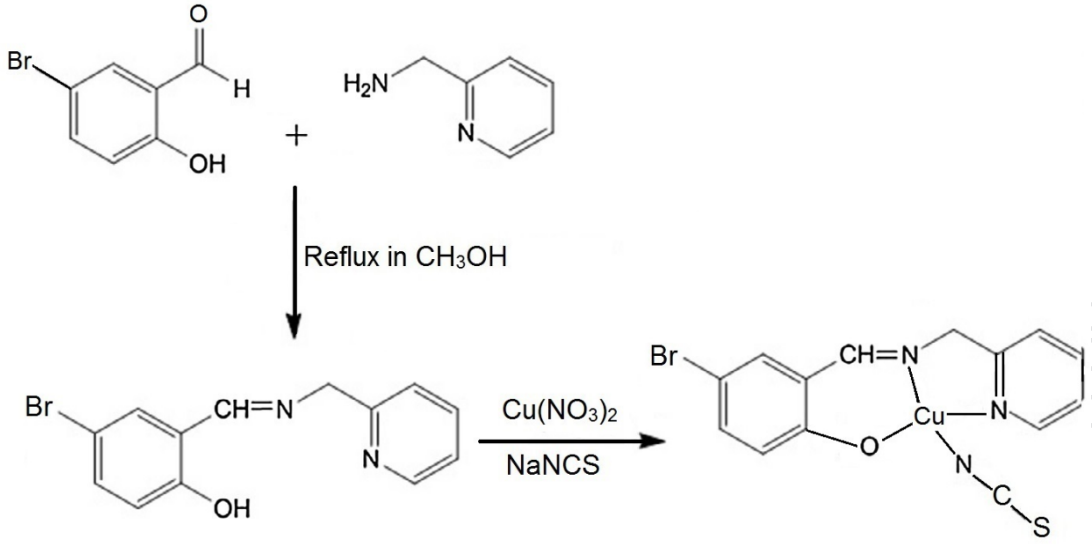
Br
O
H
OH
+
H2N
N
Reflux in CH3OH
Br
CH=N
N
OH
Cu(NO3)2
NaNCS
Br
CH=N
Cu
N
O
N
C
S

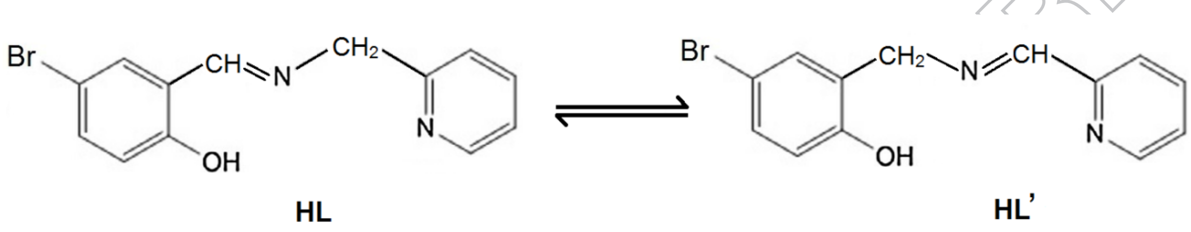
Br
CH
N
CH2
N
OH
HL
Br
CH2
N
CH
N
OH
HL'

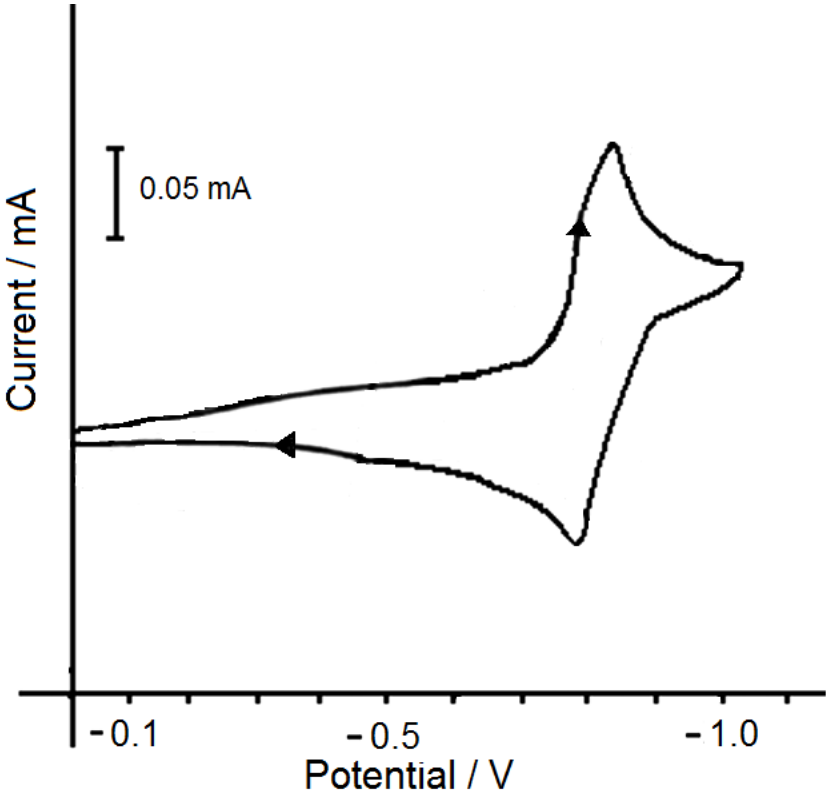
0.05 mA
Current / mA
-0.1
-0.5
-1.0
Potential / V

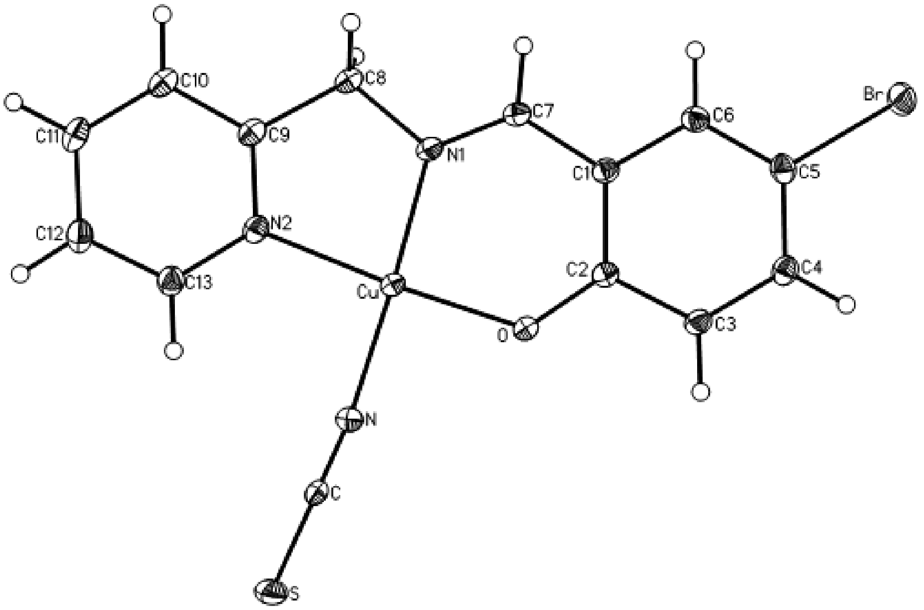
C10
C8
C7
C6
Br
C11
C9
N1
C1
C5
C12
N2
C2
C4
C13
Cu
O
C3
N
C
S

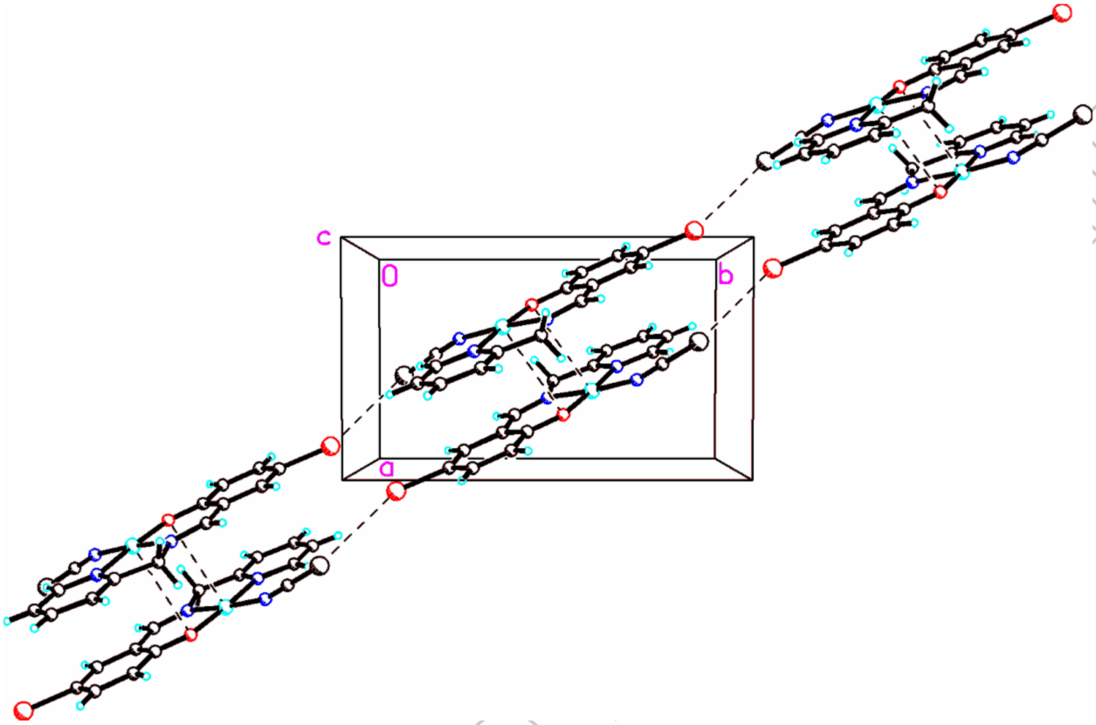
c
0
b
a

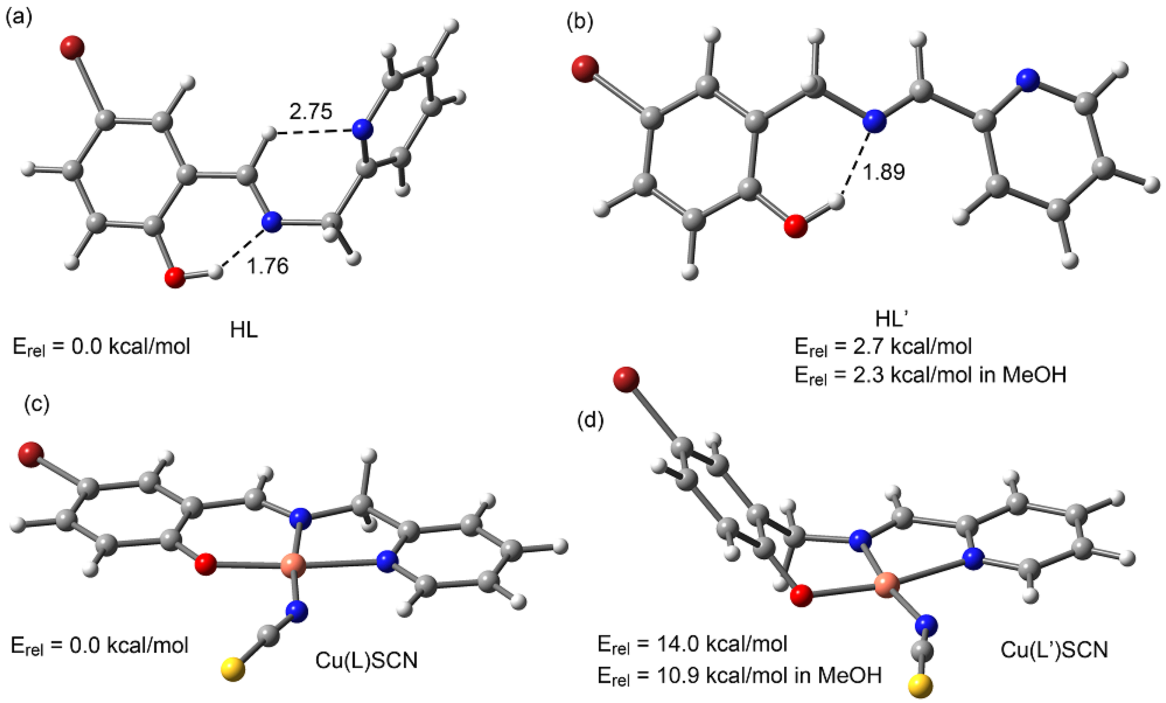
(a)
2.75
1.76
HL
E_{rel} = 0.0 kcal/mol
(b)
1.89
HL'
E_{rel} = 2.7 kcal/mol
E_{rel} = 2.3 kcal/mol in MeOH
(c)
E_{rel} = 0.0 kcal/mol
Cu(L)SCN
(d)
E_{rel} = 14.0 kcal/mol
E_{rel} = 10.9 kcal/mol in MeOH
Cu(L')SCN

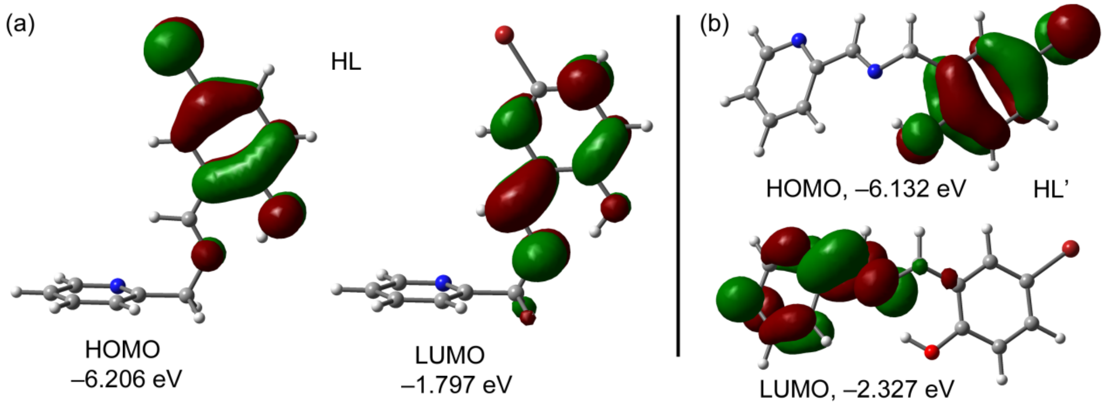
(a)
HL
HOMO
–6.206 eV
LUMO
–1.797 eV
(b)
HOMO, –6.132 eV
HL'
LUMO, –2.327 eV

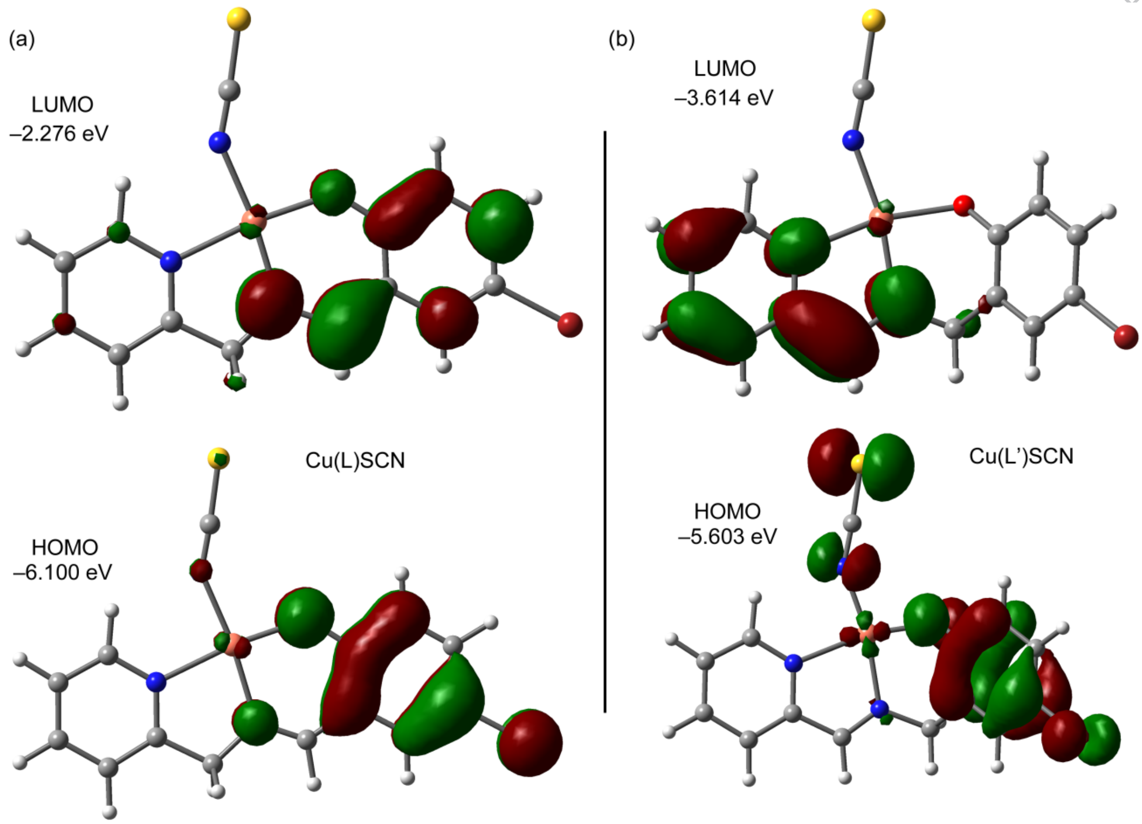
(a)
LUMO
–2.276 eV
HOMO
–6.100 eV
Cu(L)SCN
(b)
LUMO
–3.614 eV
HOMO
–5.603 eV
Cu(L')SCN